Rare Metal Materials and Engineering
Volume 51, Issue 4, April 2022
Available online at www.rmme.ac.cn

Science Press

Cite this article as: Wu Jun, Wang Li, Liu Xiao, et al. Evolution of Microstructure and Microtexture in Ti-2Al-2.5Zr During One Pass Cold Pilgering[J]. Rare Metal Materials and Engineering, 2022, 51(04): 1145-1151.

ARTICLE

Evolution of Microstructure and Microtexture in Ti-2Al-2.5Zr During One Pass Cold Pilgering

Wu Jun, Wang Li, Liu Xiao, Liao Jingjing, Wang Hui

Science and Technology on Reactor Fuel and Materials Laboratory, Nuclear Power Institute of China, Chengdu 610213, China

Abstract: The evolution of deformation behavior and microtexture in one pass cold Pilgering process was investigated. Results show that during cold Pilgering, the $\{10\bar{1}2\}$ tensile twin and prismatic slip are the two modes that are most easily activated. The activated $\{10\bar{1}2\}$ tensile twins cause the grain orientation changes in axial directions, which changes from $<10\bar{1}0>$ to $<11\bar{2}0>$. The maximum intensity point of {0001} pole figure changes along the TD, which is attributed to twinning and slip under different transient *Q*-value and equivalent plastic strain.

Key words: titanium alloy; texture; cold Pilgering; twining; deformation mode

Ti-2Al-2.5Zr is widely used in pipeline systems of liquid hydrogen and heat-conducting tubes of steam generators[1]. Its mechanical and corrosion properties are greatly affected by the microstructure and preferred orientations of crystals. In order to improve the in-service performance of Ti-2Al-2.5Zr tubes, it is necessary to investigate the microstructure and texture evolution during cold working.

Much work has been carried out on the microstructure and texture evolution of commercially pure Ti during deformation[2-6]. Akhtar[7] and Paton[8] systematically studied the deformation twinning and suggested that $\{10\bar{1}2\}<10\bar{1}0>$ tensile twinning and $\{11\bar{2}2\}<\bar{1}\bar{1}23>$ compressive twinning are dominant at room temperature. Philippe[9] and Calnan[10] pointed that twinning plays an important role in texture formation of titanium. In order to study the influence of twins on texture, Chun[6] further analyzed the evolution of twins and texture during different levels of deformation. For low and intermediate rolling reductions, twinning causes the basal pole to continuously deviate from the normal direction and turn to the transverse direction. But Deng[11] found that the basal pole changes from transverse direction to radial direction due to the combination of prismatic and pyramidal slip at low strain during cold Pilgering. The difference in texture development is attributed to the effect on the activation of deformation mechanism. Although meaningful studies on microstructure and texture evolution of cold rolling already exist, comprehensive and further studies for describing the single pass cold Pilgering remain limited, such as deformation behavior, equivalent plastic strain, and *Q*-value.

In this study, microstructure and microtexture evolution of Ti-2Al-2.5Zr was studied during one pass cold Pilgering with different *Q*-values. Electron backscattering diffraction (EBSD) was used to investigate the evolution of deformation behavior and related texture, which is important to decipher the limiting parameters and optimize the process.

1 Experiment

The as-received Ti-2Al-2.5Zr tubes, with dimensions of *Φ* 50 mm×9 mm and *Φ*36 mm×7 mm, were produced by cold Pilgering and annealing. The main chemical composition is given in Table 1. To investigate the deformation behavior and textural evolution during one pass cold Pilgering, the as-received tubes were cold-rolled from *Φ*50 mm×9 mm to *Φ*36 mm×5.5 mm (Tube A) and from *Φ*36 mm×7 mm to *Φ*25mm×5.5mm (Tube B). In order to describe the arbitrary instant before and after deformation, the transient *Q*-value and equivalent plastic strain ε_e can be defined as follows:

$$Q = \frac{\ln(t_0/t_1)}{\ln(d_0/d_1)} = \frac{\varepsilon_r}{\varepsilon_\theta} \quad (1)$$

Received date: April 03, 2021
Foundation item: Sichuan Science and Technology Program (2019ZDZX0001)
Corresponding author: Wang Hui, Ph. D., Professor, Science and Technology on Reactor Fuel and Materials Laboratory, Nuclear Power Institute of China, Chengdu 610213, P. R. China, E-mail: qinghe5525@163.com

Tabe 1 Main chemical composition of Ti-2Al-2.5Zr (wt%)

Al	Zr	Fe	Si	C	N	O	H	Ti
2.20	2.35	0.25	0.12	<0.07	<0.04	<0.13	<0.006	Bal.

$$\varepsilon_e = \sqrt{\frac{2}{3}(\varepsilon_r^2 + \varepsilon_\theta + \varepsilon_l^2)}\,\varepsilon_l \quad (2)$$

where t_0, t_1 and d_0, d_1 are the wall thicknesses and outer diameters of the tube before and after deformation, respectively; ε_r, ε_θ and ε_l are the principal strains, i.e. radial strain, tangential strain, and axial strain, respectively.

As shown in Fig. 1, samples were obtained from different positions of the tapered tube. Then a cuboid sample was cut from the middle of the block. The relevant parameters of the samples are shown in Table 2. The axial, tangential and radial directions are denoted as AD, TD and RD, respectively. Since the central zone of AD-RD plane can better reflect the rolling deformation of the sample, AD-RD observational plane of samples was mechanically ground followed by electrolytic polishing (60vol% CH_3OH+34vol% $CH_3(CH_2)_3OH$+6vol% $HClO_4$ solution, 30 V, −30 °C) in order to obtain high surface quality to meet the requirements for EBSD measurement. The microstructure was characterized on the AD-RD plane by scanning electron microscope-electron back-scattered diffraction (SEM-EBSD, FEI® Quanta 450) with Channel 5 software.

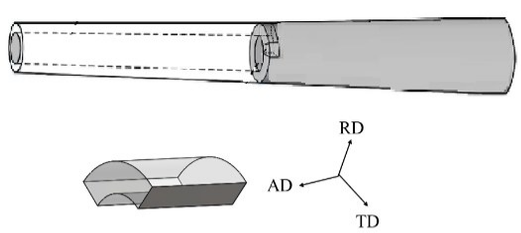

Fig.1 Sampling position of tapered tube

Table 2 Relevant parameters of samples

Parameter	Tube A			Tube B		
	S52	S53	S54	S32	S33	S34
Q	1.65	1.18	1.07	0.78	0.85	0.75
ε_e	0.92	0.98	1.03	0.81	0.93	0.98

2 Results and Discussion

2.1 Initial texture and microstructure

Fig.2 shows that initial structure of tube A and tube B after annealing consist of equiaxed grains with an average grain size of ~15 and ~13 μm, respectively. As can be seen from Fig. 2a, the red color dominates the map, which indicates that the *c*-axis of most grains is nearly parallel to TD for *Φ*50 mm×9 mm tube. It is demonstrated in Fig. 2c that (0001) pole is close to the TD, and the <10$\bar{1}$0> crystal orientation of most grains tends to coincide with AD. The main textures of the original material are {0001}//RD and <10$\bar{1}$0>//AD. While, *Φ*36 mm×7 mm tube has similar results.

2.2 Microstructure evolution during cold Pilgering

In the process of rolling deformation of single-phase α-Ti alloy, the changes in microstructure and morphology, in

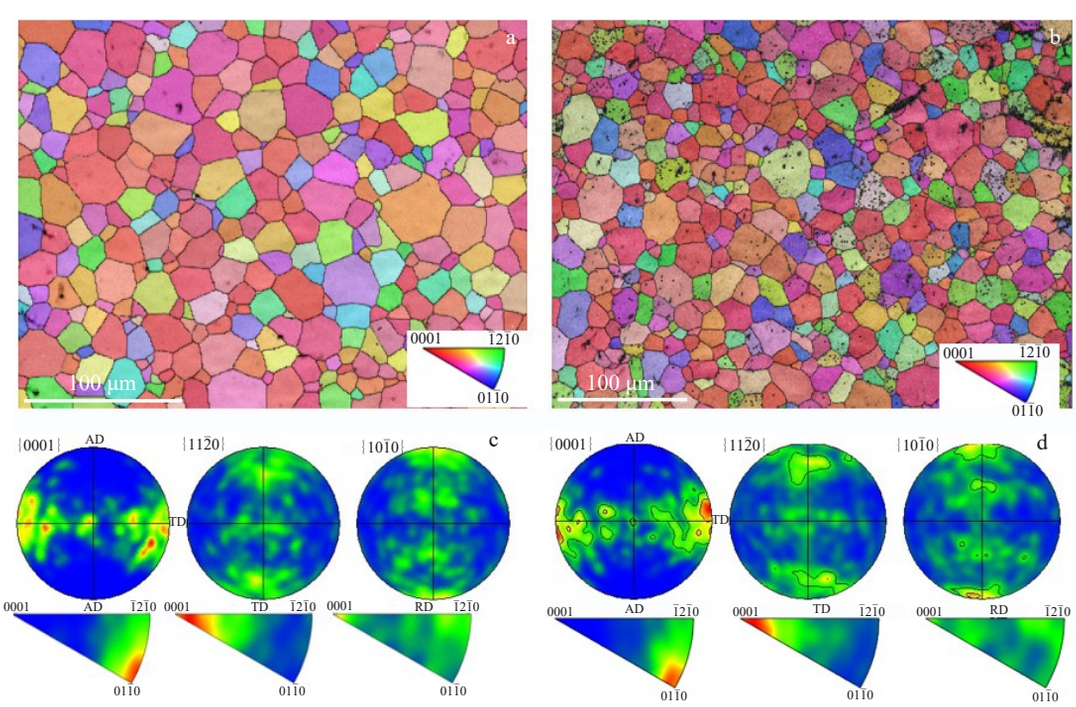

Fig.2 Initial microstructures and texture of tube A (a, c) and tube B (b, d)

addition to grain deformation, also produce twins. Because there are a lot of sub-grain boundaries in the deformed microstructure, it is difficult to observe the microstructure clearly, so only the grain boundaries with orientation angle greater than 10° are defined. Fig.3 shows the microstructure of the material under different equivalent plastic strains during rolling of tube A. When the equivalent plastic strain is 0.92, the grains are slightly elongated and a large number of twins appear in the grains. EBSD analysis shows that the twins are mainly composed of a large amount of tensile twins $\{10\bar{1}2\}$ (blue line) and a few compression twins $\{11\bar{2}2\}$ (red line). With the increase of strain, the grains continue to deform, showing a further elongated trend along the rolling direction. The grains with orientation gradient gradually increase with the increase of strain, which is related to the slip of dislocations and its aggregation near grain boundaries. The elongated grains have a higher average misorientation angle and a larger orientation gradient, indicating that the grains have a greater dislocation density. When the equivalent plastic strain reaches 1.03, the grains are seriously elongated and broken. Fig.4 shows the microstructures of the material under different equivalent plastic strains during rolling of tube B. Similarly, tube B also shows the same tendency in grain deformation and twinning. It is worth noting that the red grains in Fig.3 and Fig.4 are more easily to break. The *c*-axis of the red grains is parallel to the TD, which means that the grains in TD are more difficult to rotate during the deformation of the tube. This phenomenon is also found in the cold Pilgering process of Zr alloy pipes[11].

In both tube A and tube B, it is found that twins mainly appear in the grains whose (0001) axis tends to be parallel to the TD. For tube A, the radial strain is dominant when the Q>1. The *c*-axis of the red grains is nearly perpendicular to the radial force axis, so the grains are subjected to compressive stress perpendicular to the *c*-axis to induce tensile twins. Similarly, the red grains of tube B are subjected to tensile stress along the *c*-axis, resulting in tensile twins. There are no $\{11\bar{2}1\}$ tensile twins in tube A and tube B, mainly because $\{10\bar{1}2\}$ twins have a lower CRSS value and are easier to be activated during deformation. This experimental phenomenon also exists widely in the process of titanium alloy processing[12,13].

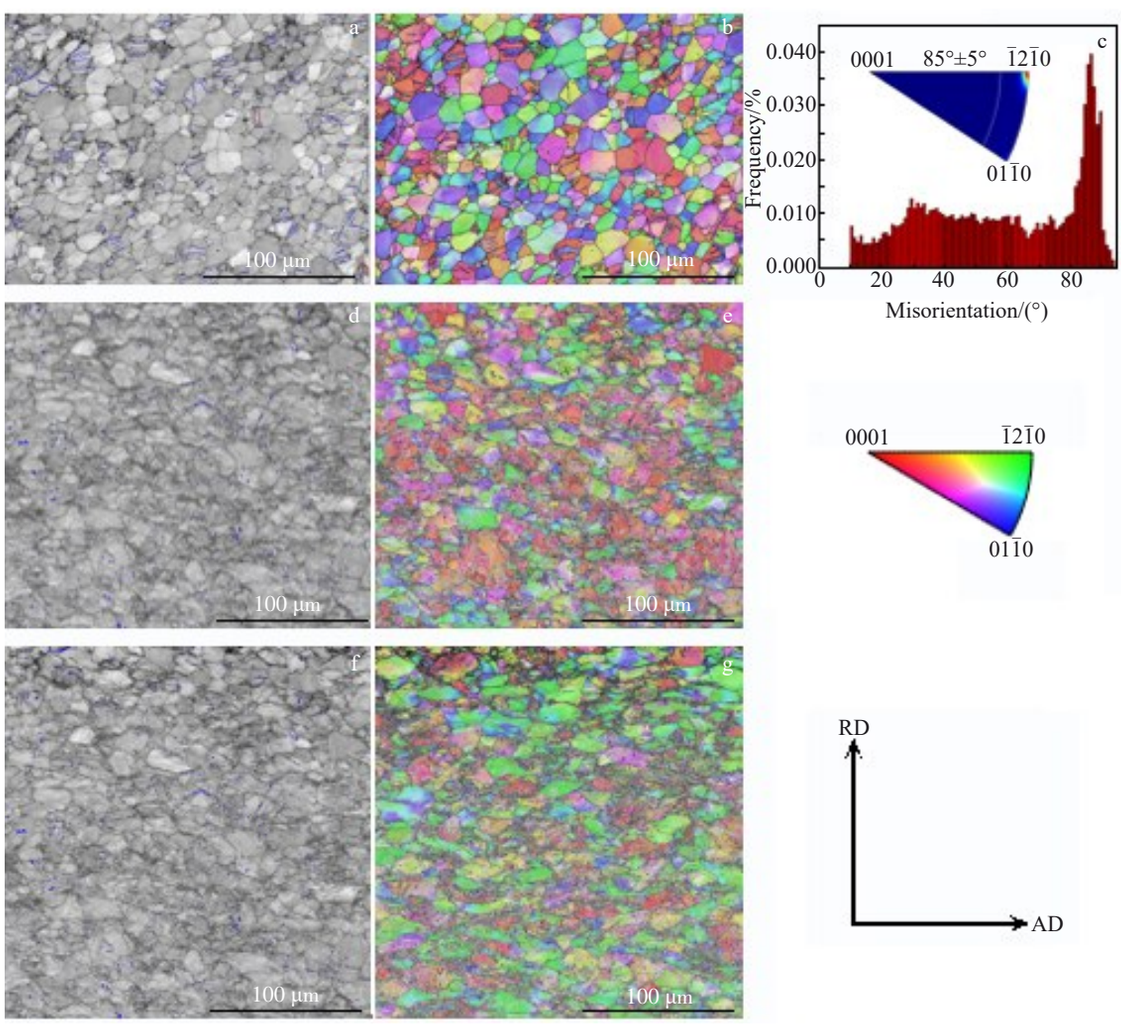

Fig.3 Microstructures of tube A samples: (a~c) S52, (d, e) S53, and (f, g) S54

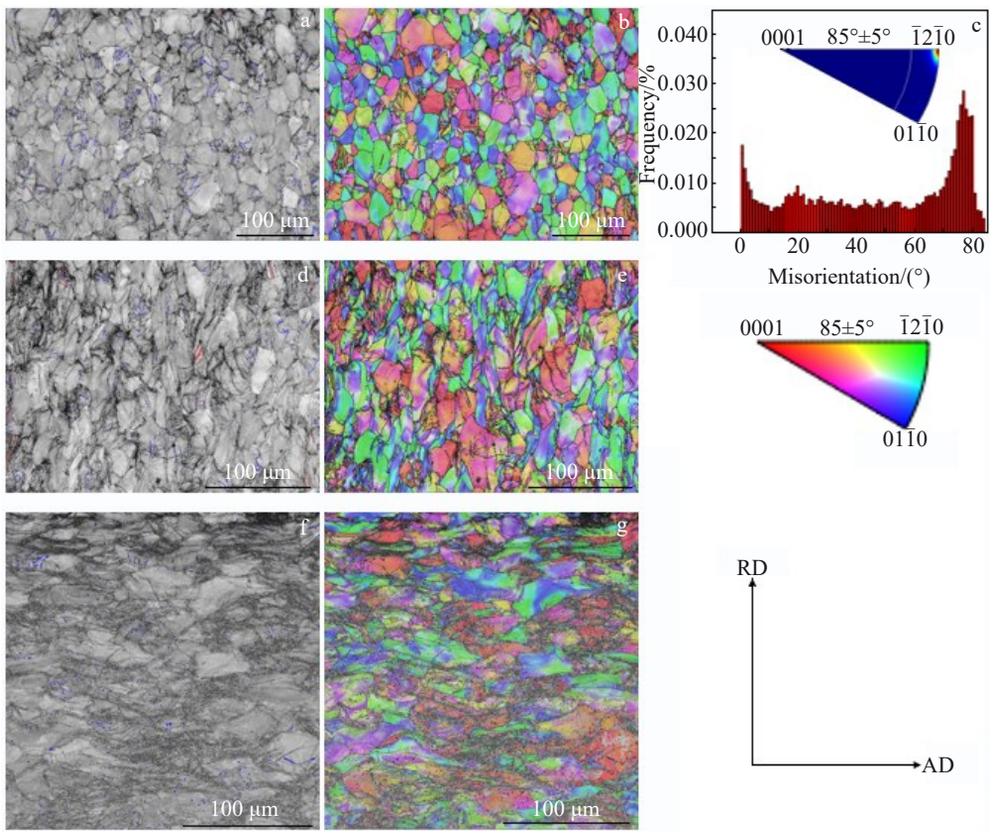

Fig.4 Microstructures of tube B samples: (a~c) S32, (d, e) S33, and (f, g) S34

2.3 Determination of slip activity

In order to verify the slip activity under different equivalent plastic strain in cold Pilgering process, the IGMA distribution method was used to analyze the slip mode activated in single grains. IGMA assumes that the rotation direction of the lattice of all crystallographic planes around the Taylor axis caused by slip is at the low indices direction within the slip plane and perpendicular to the slip direction[14]. The activation of slip modes can be determined by matching Taylor axis to IGMA. The deformation modes and standard unit triangle are shown in Fig.5. Fig.6 shows the IGMA distribution of selected grains with equivalent plastic strain ε_c of 0.81. The angle between the *c*-axis and TD through grain a~d is 9°, 78°, 54°, 63°, respectively. The distribution of grain in Fig. 6a with an orientation is closer to TD, but grain b is closer to RD. The maximum intensity of all grains at <0001> axis is greater than 2 mud. Compared with Fig.5, it can be inferred that the active slip system is prismatic <*a*> slip. The diffusion of IGMA intensity around <0001> is caused by the coactivation of other slip modes, such as pyramidal <*c*+*a*> slip. The maxima for grain c spreads away compared to grain d, so it can be deduced that the prismatic <*a*> slip is suppressed and active of other slip. This characteristic is also found in the sample with the equivalent plastic strain of 0.92. As can be seen from Fig.7, the maxima of grain f and h deviate from <0001> axis. It is obvious that the slip of pyramidal <*a*> slip is activated in grain h. The enhancement of other slip modes and the interaction between them make the distribution of IGMA more uniform, which also cause the Taylor axis to deviate from the ideal position. As reported in Ref. [11, 16], the

Deformation mode	Number of slip system	Taylor axis	Number of taylor axis
$\{1\bar{1}00\}<11\bar{2}0>$	3	<0001>	1
$\{0001\}<11\bar{2}0>$	3	$<\bar{1}0\bar{1}0>$	3
$\{1\bar{1}01\}<11\bar{2}0>$	6	$<10\bar{1}2>$	6
$\{1\bar{1}01\}<\bar{1}2\bar{1}3>$	12	$<58\bar{1}\bar{3}3>$	12
$\{1\bar{2}11\}<\bar{1}2\bar{1}3>$	12	$<51\bar{6}3>$	12

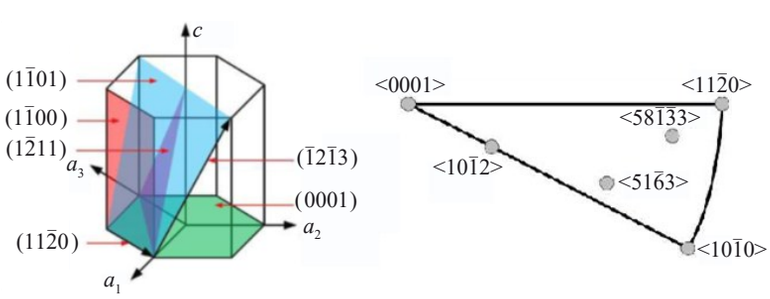

Fig.5 Deformation modes and standard unit triangle on which the Taylor axes of slip systems are available in α-Ti alloys[15]

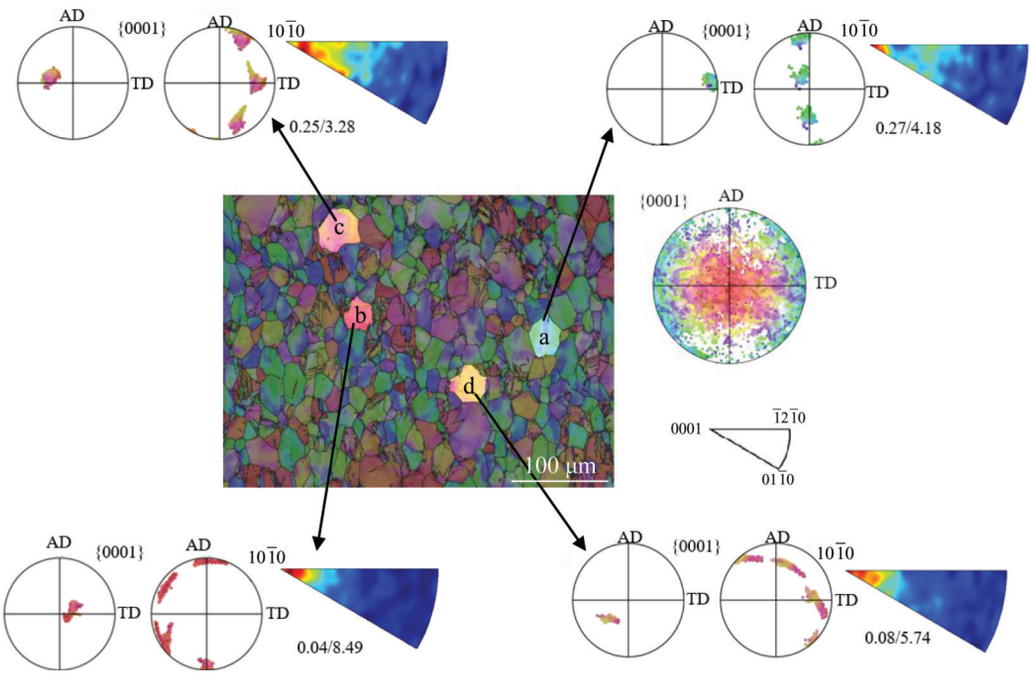

Fig.6 EBSD analysis of IGMA at ε_e=0.81

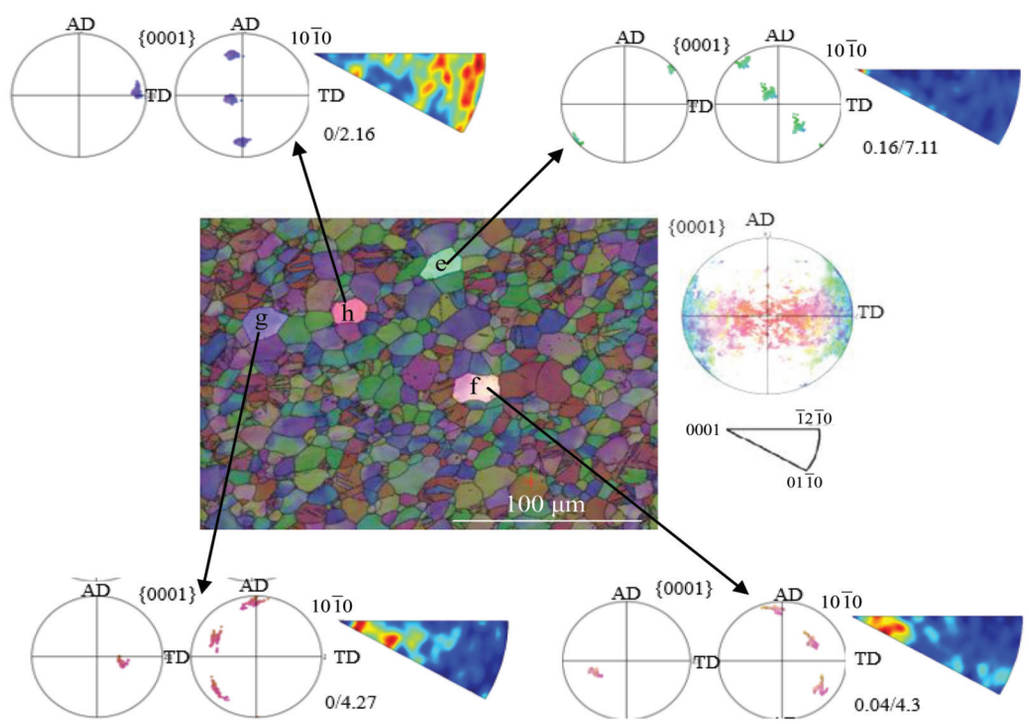

Fig.7 EBSD analysis of IGMA at ε_e=0.92

different base slip variants will result in the arc distribution of IGMA. According to this feature, it can be deduced that the distribution of intensity along <*uvt*0> axes in grain g can be interpreted as the activation of basal slip.

At the initial stage of deformation, the prismatic slip is activated preferentially due to its lowest CRSS value. With the further increase in deformation, the accumulation and pile-up of dislocations lead to the increase of local stress, which induces the generation of $\{10\bar{1}2\}$ twins in the grains with orientation advantage to accommodate the *c*-axis strain. The relationship between prismatic slip and the formation of $\{10\bar{1}2\}$ twins has been verified by relevant studies[17-19]. With

further increase of strain, more slip systems are activated to release local stress concentration and coordinate *c*-axis strain.

2.4 Microexture evolution

In the cold Pilgering process of HCP metal tube, the fracture ductility of the tube is often improved by increasing the radial texture factor[20]. The rotation of grains at TD and AD has an important effect on the radial texture factor. Fig. 8 shows the evolution of texture and the rotation of grains at AD during cold Pilgering of tube A and tube B. For tube A, when the equivalent plastic strain is 0.92, the grain tends to shift from TD to RD, but the maximum intensity point tends to TD. With the increase in equivalent plastic strain to 0.98, the tendency of grain rotation towards RD is more obvious and the maximum intensity point also turns to RD. When the equivalent plastic strain reaches 1.03, the grains turn to TD again and the maximum strength point turns to TD. For tube B, only when the equivalent plastic strain becomes 0.85, the grains tend to rotate towards RD. With the increase of strain in tube A and tube B, the grains along AD change form <10$\bar{1}$0> direction to <11$\bar{2}$0> and <10$\bar{1}$0> directions. The change of grain rotation tendency is the result of twinning and slip.

In order to clarify the influence of twins on the change of maximum intensity point in {0001} pole figure, the grains a, b, c and d were extracted from EBSD analysis diagrams of S52 and S32 samples, as shown in Fig.9. As can be seen from Fig. 9, when the grain orientation is close to TD, the twin orientation is close to RD. When the grain orientation is close to RD, the twin orientation are close to TD. For tube A, when equivalent plastic strain reaches 0.92, the movement of the maximum strength point is mainly due to a large number of twins. This also can be confirmed by the change of grain orientation from <10$\bar{1}$0> direction to <11$\bar{2}$0> direction in its reverse pole figure at AD. The orientation change caused by the twins at AD improves the capacity to accommodate strain during the deformation process, which is conducive to further deformation. With the increase in strain, the twins gradually saturate, and the initiation of other slip systems like basal slip makes the grains rotate further. However, the decrease in the *Q*-values increases the strain at TD and decreases it at RD, which causes the grains to deflect towards TD. When *Q* is close to 1, the randomness of grain rotation increases. So the maximum intensity point turns to TD. In tube B, the transient *Q*-value changes from 0.78 to 0.85 and finally to 0.75, the strain along the RD of the tube also shows a change from increasing to decreasing. The influence of transient *Q*-value on the texture and maximum strength point in the tube A and tube B is mainly related to the corresponding strain ratio. This correlation result is verified by related simulations[21].

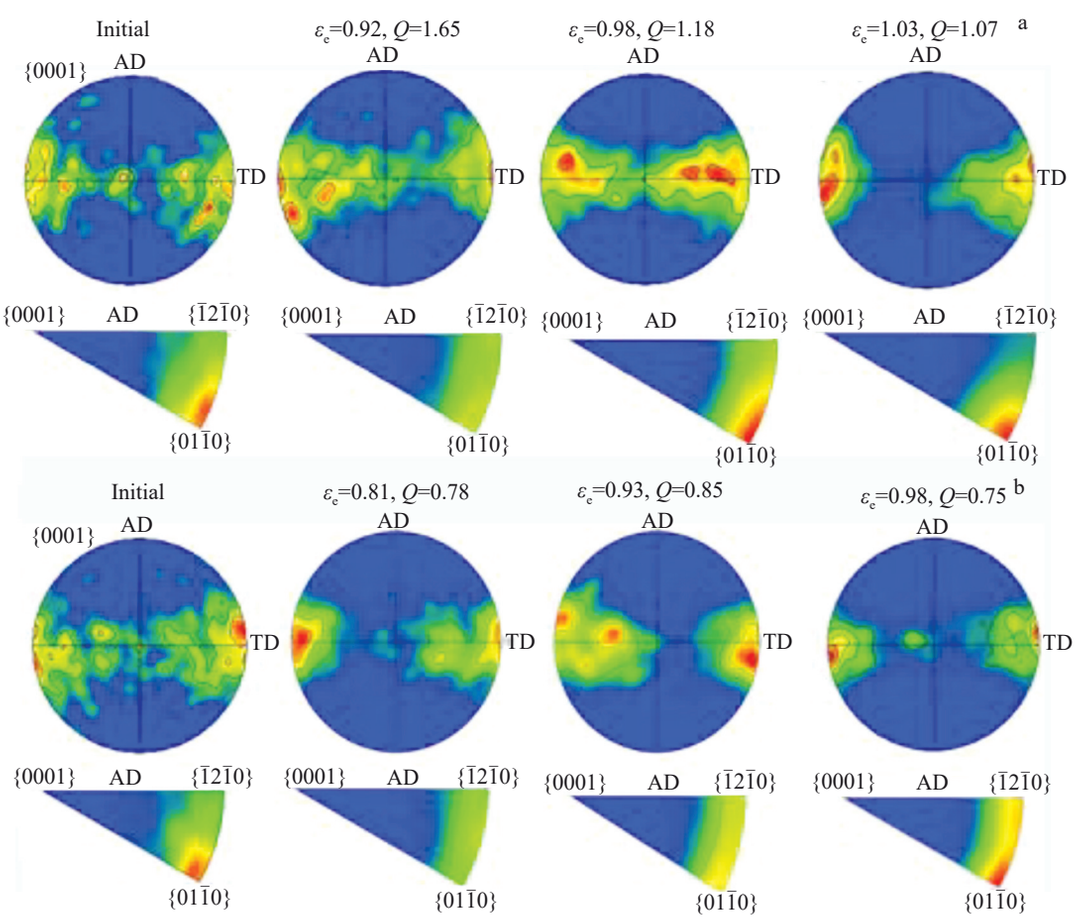

Fig.8 Texture evolution during cold Pilgering for tube A (a) and tube B (b)

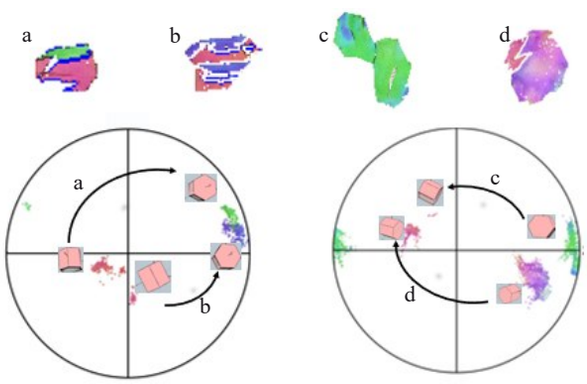

Fig.9 Orientation change of {10$\bar{1}$2} twins in {0001} pole figure for grains a, b, c, and d

3 Conclusions

1) During the cold Pilgering process of Ti-2Al-2.5Zr tubes, {10$\bar{1}$2} tensile twins and prismatic slip are the main deformation modes. As the strain increases, other slip systems are gradually activated, such as pyramidal slip.

2) The activated {10$\bar{1}$2} tensile twins cause the grain orientation change in axial directions, which rotates towards <11$\bar{2}$0> direction.

3) The changes of maximum intensity point in {0001} pole figure along the TD can be attributed to twinning and slip under different transient *Q*-value and equivalent plastic strains.

References

1 Yu Zhentao, Zhou Lian. *Rare Metal Materials and Engineering* [J], 2000, 39(2): 86 (in Chinese)

2 Bozzolo N, Dewobroto N, Wenk H R *et al. Journal of Materials Science*[J], 2007, 42(7): 2405

3 Zeng Z, Zhang Y, Jonsson S. *Materials & Design*[J], 2009, 30(8): 3105

4 Stolyarov V V, Zhu Y T, Lowe T C *et al. Nanostructured Materials*[J], 1999, 11(7): 947

5 Semiatin S L, DeLo D P. *Materials & Design*[J], 2000, 21(4): 311

6 Chun Y B, Yu S H, Semiatin S L *et al. Materials Science and Engineering A*[J], 2005, 398(1-2): 209

7 Akhtar A. *Metallurgical Transactions A*[J], 1975, 6(5): 1105

8 Paton N E, Backofen W A. *Metallurgical Transactions*[J], 1970, 1(10): 2839

9 Philippe M J, Esling C, Hocheid B. T*extures and Microstructures* [J], 1988, 7(4): 265

10 Calnan E A, Clews C J B. *Philosophical Magazine*[J], 1951, 42(331): 919

11 Deng Siying, Song Hongwu, Zheng Ce *et al. Materials Science and Engineering A*[J], 2019, 764: 138 280

12 Liu Na, Wang Ying, He Weijun *et al. Transactions of Nonferrous Metals Society of China*[J], 2018, 28(6): 1123

13 Akhtar A, Teghtsoonian E. *Metallurgical and Materials Transactions A*[J], 1975, 6(12): 2201

14 Chun Y B, Battaini M, Davies C H J *et al. Metallurgical and Materials Transactions A*[J], 2010, 41(13): 3473

15 Yan C K, Feng A H, Qu S J *et al. Acta Materialia*[J], 2018, 154: 311

16 Chen J W. *Thesis for Doctorate*[D]. Chongqing: Chongqing University, 2012 (in Chinese)

17 Wang J, Hoagland R G, Hirth J P *et al. Scripta Materialia*[J], 2009, 61(9): 903

18 Wang L, Eisenlohr P, Yang Y *et al. Scripta Materialia*[J], 2010, 63(8): 827

19 Wang L, Yang Y, Eisenlohr P *et al. Metallurgical and Materials Transactions A*[J], 2010, 41(2): 421

20 Lebensohn R A, Gonzalez M I, Tomé C N *et al. Journal of Nuclear Materials*[J], 1996, 229: 57

21 Li H, Wei D, Zhang H Q *et al. Journal of Materials Processing Technology*[J], 2020, 279: 116 520

Ti-2Al-2.5Zr 单道次皮尔格轧制过程中显微组织和织构的演化

吴　军，王　理，刘　肖，廖京京，王　辉

(中国核动力研究设计院 反应堆燃料及材料重点实验室，四川 成都 610213)

摘　要：研究了单道次皮尔格轧制过程中Ti-2Al-2.5Zr材料的变形行为和织构的演变规律。结果表明，在轧制过程中，{10$\bar{1}$2}孪晶和柱面滑移是最容易被激活的2种变形模式，{10$\bar{1}$2}孪晶的产生使得晶粒在轴向上的位向从<10$\bar{1}$0>转向<11$\bar{2}$0>。并且，在不同瞬时*Q*值和等效应变量下，滑移和孪生导致{0001}极图中最大极密度点在切向上发生变化。

关键词：钛合金；织构；皮尔格冷轧；孪晶；变形模式

作者简介：吴　军，男，1991年生，博士生，中国核动力研究设计院反应堆燃料及材料重点实验室，四川 成都 610213，电话：028-85903692，E-mail：wujunscu@163.com